

Micellar Structures of PAAm-*b*-PEO-*b*-PAAm Triblock Copolymers: Formation, Morphology, and Application as Drug Carriers

T.B. Zheltonozhskaya^{1,*}, S.V. Partsevskaya^{1,†}, D.O. Klymchuk^{2,‡}

¹ Kiev National Taras Shevchenko University, Faculty of Chemistry, Department of Macromolecular Chemistry, 60 Vladimirskaya St, 01033 Kiev, Ukraine

² Institute of Botany, National Academy of Sciences of Ukraine, 2 Tereshchenkivskaya St., 01601 Kiev, Ukraine

(Received 06 June 2012; published online 12 July 2012)

The micellization of asymmetric PAAm-*b*-PEO-*b*-PAAm triblock copolymers (TBCs) with increasing length of chemically complementary polyacrylamide and poly(ethylene oxide) blocks was studied using static light scattering, photography, UV-Vis spectroscopy and TEM. The formation of “hairy-type” and “flower-like” micelles was established in dilute aqueous and aqueous/ethanol solutions. The “hairy” micelles contained a “core” comprised cooperatively interacting PEO and PAAm segments and “corona” formed by unbound units of longer PAAm blocks. Appearance of the “flower-like” micelles was conditioned by insolubility of PAAm blocks. Stability of the “flower-like” micelles was higher than that of the “hairy-type” ones. Significant encapsulation of a model drug prednisolon by TBC micelles was established.

Keywords: Triblock Copolymer, Intramolecular Polycomplex, Micellization, Drug, Encapsulation.

PACS numbers: 62.23.St, 64.70.Nb

1. INTRODUCTION

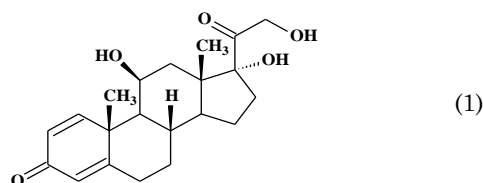
The formation and properties of block copolymer micelles in aqueous medium are intensively studied due to their application as nanoscale carriers for the encapsulation and delivering insoluble and toxic drugs [1-3]. The main attention was paid to the micelles of amphiphilic block copolymers comprised hydrophobic and hydrophilic blocks [4]. But the micelles of block copolymers with hydrophilic chemically complementary components, which form the intramolecular polycomplexes (IntraPCs) [5], are not practically studied. At the same time, these micelles are of special interest because of their enhanced binding capability in respect of different drugs and stability in competitive processes, which take place in living organisms.

In the present work, we synthesized the IntraPC-forming triblock copolymers (TBCs) such as PAAm-*b*-PEO-*b*-PAAm with hydrophilic biocompatible and partially biodegradable blocks of poly(ethylene oxide) and polyacrylamide of a variable length. Then we studied their micellization in aqueous and aqueous/ethanol solutions and encapsulation of a model poorly soluble drug prednisolon (PS) into the micellar nanocontainers.

2. EXPERIMENTAL

2.1 Materials and syntheses

Three samples of poly(ethylene glycol) (PEG) with the molecular weights $M_n = 6, 14$ and 35 kDa from “Aldrich” (USA), ammonium cerium nitrate from the same firm and acrylamide (AAM) from “Reanal” (Hungary) were applied to synthesize PAAm-*b*-PEO-*b*-PAAm triblock copolymers. A commercial PS from “Sigma Aldrich” (USA) with molecular structure (1) was used as a model drug.



The triblock copolymers were synthesized by a template radical block copolymerization of PAAm with PEG initiated by Ce^{IV} ions [5]. The reagents were mixed in the deionized water and inert atmosphere at $25\text{ }^\circ\text{C}$ for 24 h. The molar ratios $[Ce^{IV}]/[PEG] = 2$ and $[Ce^{IV}]/[AAM] = 1 \cdot 10^{-3}$ were constant in all cases. Gel-like TBCs were diluted by water, re-precipitated by acetone, dissolved again in water and freeze-dried. Chemical structure and molecular parameters of TBCs were characterized by NMR spectroscopy [6]:

Table 1 - Molecular parameters of TBCs

Copolymer	M_{nPEO} , kDa	M_{nPAAm} , kDa	M_{nTBC}^a , kDa	n^b
TBC1	6	116	238	12
TBC2	14	1045	2104	46
TBC3	35	3055	6145	54

^{a)} $M_{nTBC} = M_{nPEO} + 2 \cdot M_{nPAAm}$.

^{b)} The ratio between units of PAAm and PEO blocks.

Thus, a series of asymmetric TBCs with increasing length of both the blocks was obtained.

Also, a sample of pure PAAm with $M_v = 630$ kDa (found by viscometry) was used in our studies.

2.2 Characterization

UV spectra of PEO, PAAm, PS and polymer/PS blends in aqueous/ethanol solutions were recorded us-

* zheltonozhskaya@ukr.net

† partsevskaya@ukr.net

‡ microscopy.botany@gmail.com

ing a UV-Vis spectrometer Perkin Elmer Lambda 20 (Sweden). The turbidity (τ) of TBC and TBC/PS solutions was determined at $\lambda = 490$ nm using a LMF-72 photocolormeter from "LOMO" (Russia).

FTIR spectra of TBC, PS, and TBC/PS blend were measured using a Nexus-470 Nicolet (USA) spectrometer with a resolution 4 cm^{-1} .

Static light scattering (SLS) was used to probe the micelle formation in TBC solutions and to establish: i) the critical micellization concentration (CMC) and ii) other parameters of TBC micelles from Zimm plot [7]. For these purposes, a modernized instrument FPS-3 (Russia) contained a light-emitting diode ($\lambda = 520$ nm) from "Kingbright", an ADC-CPU™ controller from "Insoftus" (Ukraine) and the computer program WINRE-CORDER was used. To define CMC values, the scattered intensities of the vertically polarized light (I_v) were measured at the $\theta=90^\circ$ scattering angle and $T = 21^\circ \text{C}$ in a wide region of TBC concentrations. But to establish the weight-average molecular weight (M_w) of micelles, their z-average root-mean-square radius of gyration ($\langle R_g^2 \rangle_z^{1/2}$) and the second virial coefficient (A_2), the surplus scattering coefficient ($R_{v(\theta)}$) (the Rayleigh ratio [7]) was found in TBC solutions at $C > \text{CMC}$ as a function of θ . The absolute dusty-free benzene (as a standard) and the deionized dusty-free water (as a solvent) were applied in the experiments. To find the optical constant (K) of TBC solutions, the specific refractive index increment ($\partial n/\partial C$) was measured with interferometry. The value of $\partial n/\partial C = 1.65 \cdot 10^{-4} \text{ m}^3 \cdot \text{kg}^{-1}$ in TBC3 solutions turns out practically the same as that ($\partial n/\partial C = 1.65 \cdot 10^{-4} \text{ m}^3 \cdot \text{kg}^{-1}$) in PAAm solutions. Based on these data, the dependence of $C \cdot K/R_{v(\theta)}$ versus $\sin^2(\theta/2) + k \cdot C$ or Zimm plot (here k is the scaling factor) was constructed.

TEM images of TBC micelles were recorded with a JEM-1230 instrument ("JEOL", Japan) operating at an accelerating voltage of 90 kV. Small drops ($\sim 1 \cdot 10^{-4} \text{ cm}^3$) of TBC solutions ($C_{\text{TBC}} = 0.2 \text{ kg} \cdot \text{m}^{-3}$) in the deionized water or water/ethanol (30/70 v/v) mixture were deposited in copper grids coated with Formvar film and carbon and then were dried for ~ 0.5 -1 min in a vacuum desiccator at 20°C .

3. RESULTS AND DISCUSSION

The classical amphiphilic block copolymers of A-b-B and A-b-B-b-A types form micelles in aqueous medium due to a self-assembly of hydrophobic blocks. Morphology of these micelles, their size and aggregation number, the relative dimension of "core" and "corona", and also the stability in a solution are determined by chemical nature of block components as well as the length of hydrophobic and hydrophilic blocks [8]. In the IntraPC-forming block copolymers, "hydrophobic blocks" appear in dilute aqueous solutions owing to cooperative interactions of chemically complementary polymer chains [5]. Due to self-assembly of such "hydrophobic blocks" in water, the micellization process is developed.

3.1 Micellization of TBCs in water

We studied the micellization process in TBC solutions using photography, SLS, TEM and Vis spectroscopy. Onset of the micellization could be fixed by a significant increase in the scattered intensity since some critical concentration (Fig. 1 a):

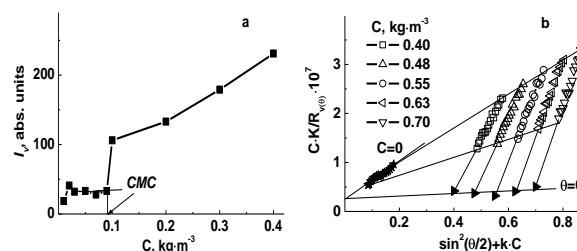


Fig. 1 – (a) Dependence of the scattered intensity vs TBC1 concentration; (b) Zimm plot for TBC3.

The CMC values and the Gibbs free micellization energies calculated by the relation: $\Delta G^\circ = RT \cdot \ln \text{CMC}$ [9] are represented in Table 2:

Table 2 - Parameters of the micellization process

Sample	CMC · 10 ⁸ , mol·dm ⁻³		-ΔG ^o , kJ·mol ⁻¹	
	H ₂ O	H ₂ O/EtOH ^{a)}	H ₂ O	H ₂ O/EtOH
TBC1	37.8	8.4	36.15	39.82
TBC2	19.0	3.8	37.83	41.76
TBC3	4.9	1.3	41.15	44.38

a) H₂O/EtOH=30/70 v/v.

The regular reduction in CMC values and the increase in $-\Delta G^\circ$ with growth of PEO (and PAAm) length indicated enhance in the micellar stability at the transition from TBC1 to TBC3. For TBC3 with the longest PEO block, additional micellar parameters: $M_w = 37686 \text{ kDa}$, $A_2 = 1.283 \cdot 10^{-5} \text{ mol} \cdot \text{m}^3 \cdot \text{kg}^{-2}$ and $\langle R_g^2 \rangle_z^{1/2} = 248.4 \text{ nm}$ were found from Zimm plot (Fig. 1 b) using the double extrapolation procedure [7]. The aggregation number $Z \approx 6$ was also estimated for these micelles using the ratio: $Z = M_w/M_n \text{TBC3}$.

Taking into account highly asymmetric character of TBC macromolecules (Table 1), the formation of "hairy-type" micelles [8] in dilute aqueous solutions could be assumed (the left part of Fig. 2). A small "core" of these micelles would contain H-bonded PEO and PAAm segments but a large "corona" would comprise the surplus unbound segments of PAAm.

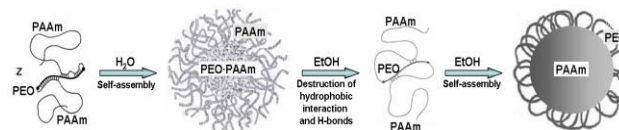


Fig. 2 – A scheme of TBC micellization in water and micelle transformations at ethanol addition.

Real morphology of TBC1 and TBC3 micelles in water solutions is shown in TEM images (Fig. 3 a, c). It is seen that TBC1 macromolecules form mainly spherical "hairy" micelles (Fig. 3 a), while morphology of TBC3 micelles is more multifarious. In addition to relatively small spherical micelles the image in Fig. 3 c demonstrates also "cubic-like" (or "plate-like") micellar structures. On average, their size is some higher than that of TBC1 micelles. The appearance of such unusual micelles could be explained by the formation of their "cores" by rigid "hydrophobic blocks" of TBC3, which ones contain (unlike to TBC1) more lengthy sequences of H-bonded units of PAAm and PEO. Displaying small dark spots throughout TEM images in Fig. 3 a, c is of

special interest. This fact indicates the presence in TBC solutions together with large polymolecular micelles also small monomolecular micelles, which are individual IntraPCs shown in Fig. 2.

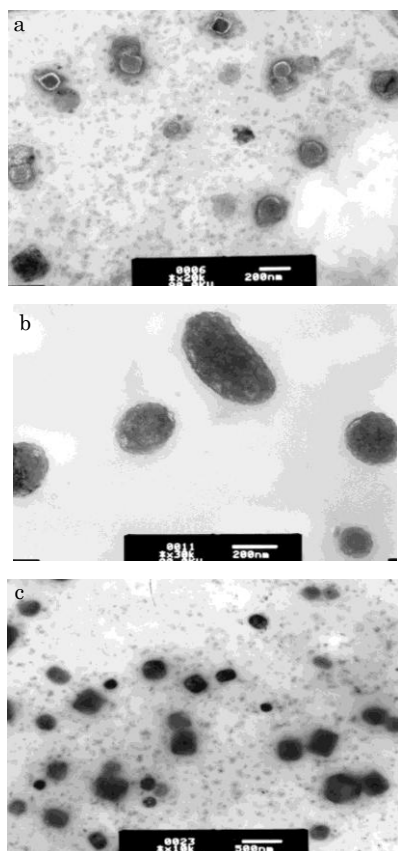


Fig. 3 – TEM images of (a, b) TBC1 and (c) TBC3 micelles prepared in (a, c) aqueous and (b) aqueous/ ethanol (30/70 v/v) solutions. $C_{TBC} = 0.2 \text{ kg}\cdot\text{m}^{-3}$

3.2 Micellization of TBCs in the mixed solvent

The addition of ethanol up to $\sim 30 \text{ v}\%$ noticeably enhances the transparency of TBC solutions and reduces the scattered intensities in them. The last values remain practically unchanged in all range of concentrations under study. But at ethanol content $\geq 40 \text{ v}\%$, the turbidity of TBC solutions sharply grows (Fig. 4 a) since very low concentration (Fig. 4 b) that implies the arising new micellar structures.

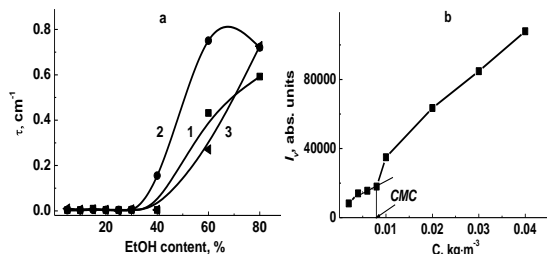


Fig. 4 – (a) The turbidity of TBC1 -1, TBC2 -2 and TBC3 -3 solutions vs EtOH content ($C_{TBC} = 0.4 \text{ kg}\cdot\text{m}^{-3}$); (b) the example of CMC determination for TBC3 in aqueous/ethanol (30/70 v/v) solution. $T = 21 \text{ }^\circ\text{C}$.

We interpreted this picture by influence of some factors. First, ethanol is capable of destroying hydrophobic

interactions in a micellar “core”. Also, it can partially ruin H-bonds between PAAm and PEO because of competitive interactions with functional groups of the blocks. These factors act at small ethanol percent and lead to destruction of initial “hairy” micelles (a central part of Fig. 2). Further, pure ethanol is insolvent in respect of PAAm chains. Therefore, an intense micellization of TBCs at high ethanol percent is developed due to insolubility of PAAm blocks. In this case, the appearance of the “flower-like” micelles would be waiting (the right part of Fig. 2) [10]. Insoluble “tails” of PAAm would form a large micellar “core”, while soluble “loops” of PEO would be concentrating in a “corona”. According to CMC and $-\Delta G^\circ$ values in Table 2, the “flower-like” micelles in aqueous/ethanol solutions are more stable than “hairy” ones in water. Such result is conditioned by essentially larger length of PAAm chains as compared to PEO block.

A real view of the “flower-like” micelles is shown in Fig. 3 b. It is seen that they possess as spherical as elongated (spheroid) shape. Moreover, their size (for TBC1) is higher than that of the “hairy-type” micelles obtained in water (Fig. 3 a, b).

3.3 Encapsulation of the model drug

The supplement of PS changed a micellization picture in TBC water/ethanol solutions that was reflected in the turbidity curves and photos (Fig. 5).

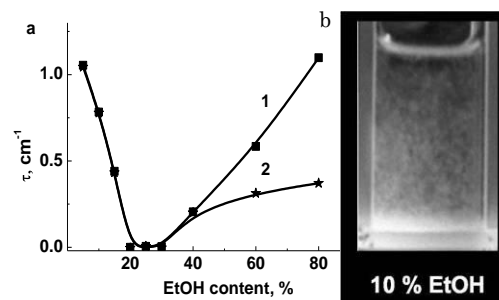


Fig. 5 – (a) The turbidity of TBC3/PS solutions -1 vs EtOH content ($C_{TBC} = 0.4 \text{ kg}\cdot\text{m}^{-3}$, the ratio $\phi = 0.64 \text{ mol}/\text{base-mol}_{TBC}$); (b) a photo of TBC3/PS solution at EtOH content of 10 v %. The difference -2 (a) between turbidity curves ($\tau_{(TBC3/PS)} - \tau_{TBC} = f[\text{EtOH}]$).

At small ethanol percent (up to 20 v %) we observed a high turbidity in TBC/PS solutions (Fig. 5 a, curve 1) caused by the formation of “snow-flakes-like” micellar structures (Fig. 5 b), which were absent in PS-free solutions (Fig. 4 a). Also, an additional increase in the turbidity caused by PS introduction occurred at ethanol content $\geq 40 \text{ v}\%$ (Fig. 5 a, curve 2). This indicated the interaction of PS with TBCs, which initiated the changes in the “hairy-type” micelles at small ethanol percent and intensified the micelle formation at high ethanol content.

The drug molecules (structure (1)) contain two carbonyl and three hydroxyl groups, which are capable of forming H-bonds with proton-donor and proton-acceptor groups of TBCs. Therefore, we studied H-bonding in TBC/PS blend by FTIR and UV spectroscopy. In the last case we analyzed the changes in UV spectrum of PS in two solvents ($\text{H}_2\text{O}/\text{EtOH} = 70/30$ and $30/70 \text{ v/v}$) under the effect of PEO and PAAm separate-

ly (Fig. 7 a, b). In both solvents a similar picture was observed: PEG did not change the position ($\lambda_{\max} = 247$ nm) and intensity of $n \rightarrow \pi^*$ transition (Fig. 7 a), while PAAm presence led to the lowering the transition intensity (Fig. 7 b). This result confirmed the existence of weak H-bonds [11] between PS carbonyls and $-\text{NH}_2$ fragments of PAAm amide groups in both the solvents.

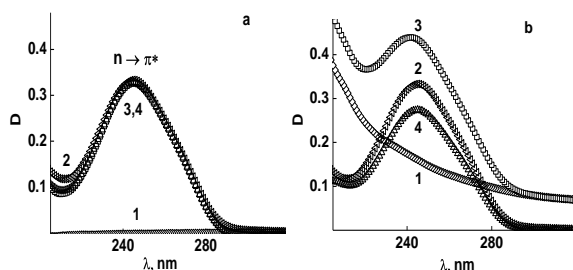


Fig. 6 – UV spectra for: PEG3 –1 (a), PAAm –1 (b), PS –2 (a, b), PEG3/PS –3 (a) and PAAm/PS –3 (b) in water/ethanol (30/70) solutions, and the differences ($D_{\text{PEG3/PS}} - D_{\text{PEG3}}$) –4 (a) and ($D_{\text{PAAm/PS}} - D_{\text{PAAm}}$) –4 (b) vs λ . ($C_{\text{PEG}} = C_{\text{PAAm}} = 4 \cdot 10^{-3} \text{ kg} \cdot \text{m}^{-3}$, $C_{\text{PS}} = 8.53 \cdot 10^{-3} \text{ kg} \cdot \text{m}^{-3}$).

Participation of $-\text{OH}$ groups of PS in H-bonding with TBCs was confirmed by FTIR (the data are not shown). The main effect consisted in the appearance of new intense band of $\nu_{\text{O-H}}$ vibrations at $\sim 3290 \text{ cm}^{-1}$ in FTIR spectrum of TBC/PS blend unlike to spectra of TBC and PS. Thus, one could be assume that the formation of “snow-flakes-like” structures in TBC solutions at PS addition developed due to H-bonding drug molecules with PAAm and PEO blocks followed by hydrophobic segregation of the bound segments.

Characterization of PS encapsulation by the TBC “hairy” micelles was carried out in the solvent $\text{H}_2\text{O}/\text{EtOH} = 80/20$ v/v at TBC concentration $C = 1 \text{ kg} \cdot \text{m}^{-3}$, three ratios of $\phi = 0.021, 0.42, 0.60$ molPS/base-molTBC and a contact time of 24 h. The “snow-flakes-like” micellar structures were separated by a centrifugation; then PS concentration in solutions was

established by UV spectroscopy at $\lambda = 247$ nm. At the smallest $\phi = 0.021$ an essential clouding of TBC1-3 solutions was not observed. Therefore, in these cases it was impossible to separate the products of TBC interaction with PS and to determine the quantity of bound drug. The results for other two PS/TBC ratios are collected in Table 3.

Table 3 – PS encapsulation by “hairy” micelles

Copolymer	ϕ , molPS/base-molTBC	$X_{\text{PS}}^{\text{a)}$, wt %
TBC1	0.42	8.8
	0.60	48.5
TBC2	0.42	8.5
	0.60	55.6
TBC3	0.42	17.8
	0.60	56.8

^{a)} The degree of PS encapsulation.

It is seen a drastic enhance in PS content in the “snow-flakes-like” micelles with ϕ growth and a small increase in that at the transition from TBC1 to TBC3.

CONCLUSION

The asymmetric triblock copolymers PAAm-*b*-PEO-*b*-PAAm with chemically complementary blocks formed the “hairy-type” micelles in aqueous medium. Their stability grew with increase in the length of PEO (and PAAm) blocks. Morphology of the micelles was changed from spherical shape for TBC1 to the mixture of spherical and “cubic-like” (or “plate-like”) structures for TBC3. Small ethanol additives (up to ~ 30 v %) caused a gradual destruction of the “hairy” micelles, while at high ethanol percent (> 40 v %) the formation of new “flower-like” ones took place. The “hairy” TBC micelles encapsulated significant quantities of poorly soluble drug PS via hydrogen bonds and hydrophobic interactions that led to the appearance of the “snow-flakes-like” micellar structures.

REFERENCES

1. S. Svenson, In: *Carrier-based drug delivery*, Ch.1 (Washington, DC: ACS Symposium Series 879, 2004).
2. D.K. Kim, J. Dobson, *J. Mater. Chem.* **19**, 6294 (2009).
3. Y. Kim, P. Dalhaimer, D.A. Christian, D.E. Disher, *Nanotechnology* **16**, S484 (2005).
4. K. Cho, X. Wang, S. Nie, Z.(G.) Chen, D.M. Shin, *Clin. Cancer Res.* **14**, 1310 (2008).
5. T. Zheltonozhskaya, N. Permyakova, L. Momot, In: *Hydrogen-bonded interpolymer complexes. Formation, structure and applications*, Ch.5 (New Jersey-London-Singapore-Beijing etc.: World Scientific, 2009).
6. S.V. Fedorchuk, T.B. Zheltonozhskaya, E.M. Shembel, L.R. Kunitskaya, I.M. Maksuta, Yu.P. Gomza, *Functional materials* **18**, 1 (2011).
7. K. Khougaz, I. Astafieva, A. Eisenberg, *Macromolecules* **28**, 7135 (1995).
8. G. Riess, *Prog. Polym. Sci.* **28**, 1107 (2003).
9. H. Shen, L. Zhang, A. Eisenberg, *J. Phys. Chem.* **101**, 4697 (1997).
10. M.L. Gou, X.L. Zheng, K. Men, J. Zhang, L. Zgeng, X.H. Wang, F. Luo, Y.L. Zhao, X. Zhao, Y.Q. Wei, Z.Y. Qian, *J. Phys. Chem. B* **113**, 12928 (2009).
11. Yu.A. Pentin, L.V. Vilkov, *Physical methods for investigations in chemistry* (Moscow: Mir, “AST”: 2003).